Upper Guadalupian to Lower Lopingian Latentifistularian (Radiolaria) Interval Zones of the Mino Belt in the Mt. Funabuseyama Area, Central Japan

Authors: Kuwahara, Kiyoko, and Sano, Hiroyoshi

Source: Paleontological Research, 21(4) : 422-440

Published By: The Palaeontological Society of Japan

URL: https://doi.org/10.2517/2017PR004

The BioOne Digital Library (https://bioone.org/) provides worldwide distribution for more than 580 journals and eBooks from BioOne's community of over 150 nonprofit societies, research institutions, and university presses in the biological, ecological, and environmental sciences. The BioOne Digital Library encompasses the flagship aggregation BioOne Complete (https://bioone.org/subscribe), the BioOne Complete Archive (https://bioone.org/archive), and the BioOne eBooks program offerings ESA eBook Collection (https://bioone.org/esa-ebooks) and CSIRO Publishing BioSelect Collection (https://bioone.org/csiro-ebooks).

Your use of this PDF, the BioOne Digital Library, and all posted and associated content indicates your acceptance of BioOne's Terms of Use, available at www.bioone.org/terms-of-use.

Usage of BioOne Digital Library content is strictly limited to personal, educational, and non-commmercial use. Commercial inquiries or rights and permissions requests should be directed to the individual publisher as copyright holder.

BioOne is an innovative nonprofit that sees sustainable scholarly publishing as an inherently collaborative enterprise connecting authors, nonprofit publishers, academic institutions, research libraries, and research funders in the common goal of maximizing access to critical research.

Downloaded From: https://complete.bioone.org/journals/Paleontological-Research on 15 Jul 2025
Terms of Use: https://complete.bioone.org/terms-of-use

Paleontological Research, vol. 21, no. 4, pp. 422–440, October 1, 2017
© by the Palaeontological Society of Japan
doi:10.2517/2017PR004

Upper Guadalupian to lower Lopingian latentifistularian (Radiolaria) interval zones of the Mino Belt in the Mt. Funabuseyama area, central Japan

KIYOKO KUWAHARA[1] AND HIROYOSHI SANO[2]

[1]*Faculty of Clinical Education, Ashiya University, Rokurokuso-cho, Ashiya, Hyogo 659-8511, Japan (e-mail: permorads@kcn.jp)*
[2]*Department of Earth and Planetary Sciences, Kyushu University, 744 Motooka, Fukuoka 819-0839, Japan*

Received October 26, 2016; Revised manuscript accepted February 13, 2017

Abstract. We present a biostratigraphic study of the Latentifistularia (Radiolaria) in the upper Guadalupian to lower Lopingian (upper Capitanian to lower Wuchiapingian; Permian) succession of bedded chert of the Mino Belt in the Mt. Funabuseyama area, central Japan. The rocks examined are interpreted to be of the pelagic facies on the deep-marine lower flank of a mid-Panthalassic seamount. We established six latentifistularian-based interval zones in the chert succession (*ca.* 12.5 m in thickness) by using the first appearance datum of the latentifistularian species. They are the *Foremanhelena triangula*, *Ruzhencevispongus* sp. B, *Ruzhencevispongus* sp. C, *Triplanospongos angustus*, *Cauletella paradoxa*, and *Triplanospongos musashiensis* interval zones in ascending order. The first interval zone is underlain by an unnamed zone characterized by *Follicucullus charveti* and *Follicucullus* spp. with minor *F. bipartitus* and *Pseudoalbaillella* sp. On the basis of the radiolarian assemblage, we correlate the *Foremanhelena triangula*, *Ruzhencevispongus* sp. B, *Ruzhencevispongus* sp. C, *Triplanospongos angustus* interval zones and the *Cauletella paradoxa* and *Triplanospongos musashiensis* interval zones with the *Follicucullus charveti-Albaillella yamakitai* and *Neoalbaillella ornithoformis* assemblage zones in Japan, respectively. The lower three interval zones and the upper two interval zones are compared with the upper Capitanian and lower Wuchiapingian, respectively. The *Triplanospongos angustus* Interval Zone presumably includes the Guadalupian-Lopingian boundary. Our results show that the latentifistularians can be used to formulate a biostratigraphic zonation of the upper Capitanian to lower Wuchiapingian stages, in which the albaillellarians are much less abundant and diverse. The newly proposed interval zones permit the further subdivision of upper Capitanian to lower Wuchiapingian successions.

Key words: chert, interval zones, Japan, Latentifistularia, Permian

Introduction

Albaillellarians have played an important role in establishing the Permian radiolarian biostratigraphy and its international correlation. An Albaillellaria-based biostratigraphy for the Permian was first outlined in the American Cordillera by Holdsworth and Jones (1980). Soon after pioneer work by these authors, the Pennsylvanian to Permian radiolarian biostratigraphy was proposed on the basis of the stratigraphic distribution of the albaillellarian assemblages in deep-marine chert sections within the Jurassic accretionary complex of Japan (Ishiga and Imoto, 1980; Ishiga *et al*., 1982). As those sections often occur isolated from one another, the biostratigraphy was established by piecing together and correlating the stratigraphic distribution of albaillellarian fossils in each section (e.g. Ishiga, 1986). The Permian albaillellarian-based biostratigraphy by Ishiga *et al*. (1982) has been widely accepted and applied with an emendation of just the two Lopingian biozones by Kuwahara *et al*. (1998).

On the other hand, a Permian radiolarian biostratigraphic scheme based on non-albaillellarian taxa, including the Latentifistularia, Entactinaria, and Spumellaria, was proposed in pioneer work by Nazarov and Ormiston (1985). Given the availability of Permian Latentifistularia in the assemblages studied, Nazarov and Ormiston (1986b) proposed their biostratigraphic scheme based on the stratigraphic change of the latentifistularian assemblage. The latentifistularian-based biostratigraphy was, however, less widely used than the albaillellarian-based biostratigraphy, because latentifistularians are actually more difficult to identify than albaillellarians. For this reason Permian non-albaillellarian taxa have received less attention as biostratigraphic tools than the albaillellarians.

Meanwhile, additional paleontological studies concerned with the systematic description of Guadalupian and Lopingian non-albaillellarians have been conducted (e.g. Caridroit and De Wever, 1986; Feng *et al*., 2006a, b; Maldonado and Noble, 2010; Nestell and Nestell, 2010; Noble and Jin, 2010; Noble and Renne, 1990; Sashida and Tonishi, 1985, 1986, 1988; Shang *et al.*, 2001). Very well preserved specimens of non-albaillellarians reported in these studies permit easier identification and classification than before. However, their stratigraphic occurrence is sporadic, mostly from limited levels of siliceous and calcareous rock successions on Tethyan and Pangean shelves. This means that the Guadalupian and Lopingian non-albaillellarian-based biostratigraphy is difficult to establish in the western United States and south China.

Japanese bedded chert and related siliceous rocks also bear prolific Guadalupian and Lopingian non-albaillellarians. They are diverse, but much more poorly preserved when compared with the non-albaillellarians from North America and China. However, the Japanese bedded chert and related siliceous rocks retain much longer-ranging biostratigraphic successions of Guadalupian and Lopingian Permian non-albaillellarian fossils than the North American and Chinese rocks. This is due to the depositional setting of the Japanese siliceous rocks that comprise truly deep-marine and pelagic facies formed in an open-ocean realm in a mid-Panthalassic region.

This paper examines the biostratigraphic distribution of the upper Guadalupian to lower Lopingian (upper Capitanian to lower Wuchiapingian; Permian) latentifistularian species along with the Albaillellaria in a bedded chert section of the Mino Belt in Japan. Applying the systematic study in North America and China, we propose new upper Guadalupian to lower Lopingian Latentifistularia-based interval zones. Our careful examination shows that the Latentifistularia work as significant tools for biostratigraphy and correlation of upper Capitanian to lower Wuchiapingian rocks, in which the Albaillellaria is less abundant and diverse.

Geologic setting

The Mino Belt comprises a Jurassic (partly earliest Cretaceous) subduction-generated accretionary complex of unmetamorphosed oceanic and terrigenous rocks, exposed in central Japan (Mizutani, 1990). Wakita (1988) divided the accreted rocks of the Mino Belt into seven, fault-bounded tectonostratigraphic units of two coherent units and five mélange units. The former represents a deep-marine oceanic plate stratigraphy consisting of Lower Triassic siliceous claystone, Lower Triassic to lowest Cretaceous radiolarian chert and related siliceous rocks, and Upper Jurassic to lowest Cretaceous trench-fill turbiditic sediments (Wakita, 2012). The mélange units are commonly characterized by chaotic mixing of various-sized blocks of Permian to Jurassic oceanic rocks with a matrix of the intensely sheared Lower Jurassic to lowest Cretaceous mudstone (Wakita, 2012). The oceanic rocks include the Cisuralian basaltic rocks, upper Cisuralian to upper Guadalupian shallow-marine limestone and limestone breccia (Sano, 1988b, 1989a), middle Cisuralian to upper Lower Triassic chert and siliceous rocks with displaced dolomite (Sano, 1988a; Kuwahara *et al*., 2010), and Triassic to Jurassic chert (Wakita, 1988) and sandstone.

Sano (1988a) divided the Permian oceanic assemblage in the Mt. Funabuseyama area into three nearly time-equivalent stratigraphic units. Each is characterized by shallow-marine limestone, carbonate breccia, and deep-marine chert, all of which are underlain by basaltic rocks. Sano (1988b, 1989a) date the former two units as the upper Cisuralian to upper Guadalupian and the upper Cisuralian, respectively. The chert-dominant unit, designated as the Hashikadani Formation, is correlated with the middle Cisuralian to upper Lower Triassic (Sano, 1988a; Kuwahara *et al*., 2010; Sano *et al*., 2010). The Permian oceanic assemblage in the Mt. Funabuseyama area is interpreted to have accumulated on and around an oceanic seamount in a mid-Panthalassic Ocean (Jones *et al*., 1993; Safonova *et al*., 2016; Sano, 1989b; Sano *et al*., 1992).

The examined section is exposed in the upper reaches of the Iwaidani gully (loc. NF 195 in Figure 1.2) in the Mt. Funabuseyama area, central Japan (Figure 1.2). The examined upper Guadalupian to lower Lopingian bedded chert stratigraphically corresponds to the upper part of the Hashikadani Formation (Sano, 1988a).

Lithostratigraphy of study section

The chert predominantly crops out in the approximately 30-m-long, east-west extending exposure, along with black claystone and scaly mudstone (section NF 195: Figure 2). The chert beds at this locality strike northwest-southeast and are inclined to the northeast with varying angles. Exposed at the eastern end of section NF 195 is a part of a structural wedge of the Middle Jurassic scaly mudstone interleaved within the Hashikadani oceanic rocks (Figure 1).

As the examined chert in the present study is cut by several faults, we established five subsections NF 195G to NF 195C from west to east (Figure 2) and measured each separately. We then correlated subsections NF 195G

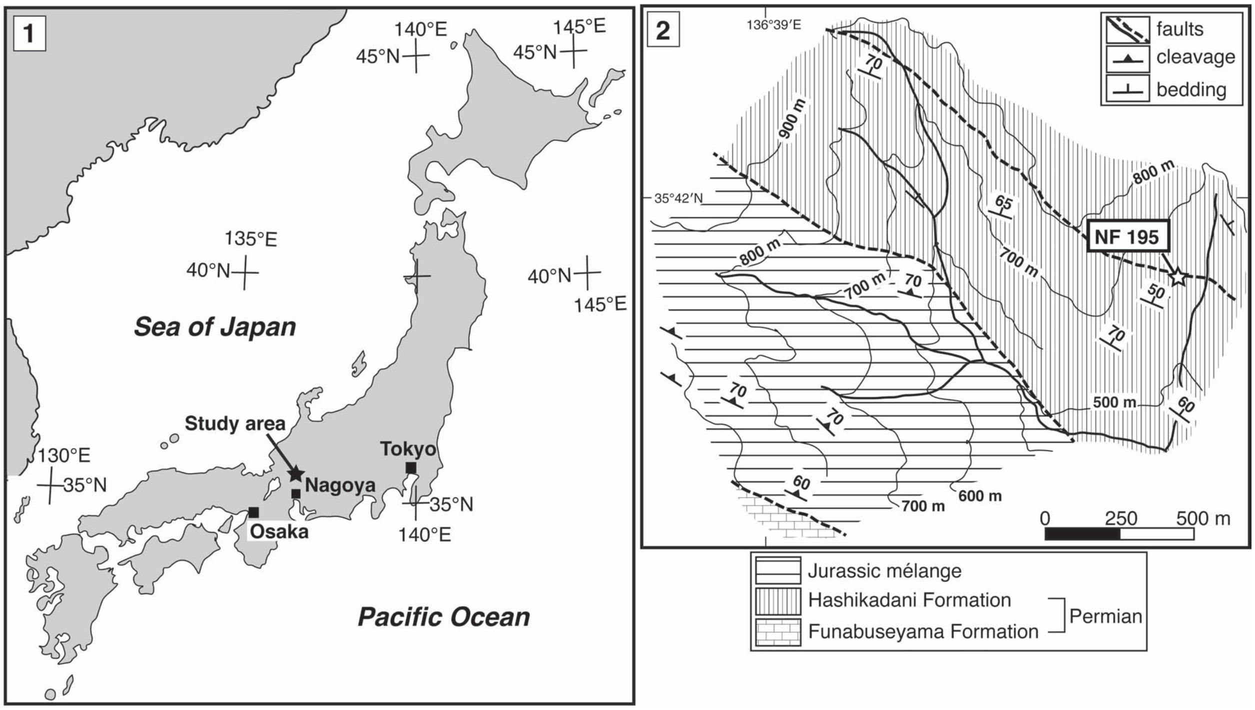

Figure 1. Maps showing (**1**) the approximate locality of the study area in central Japan and (**2**) the locality of the study section NF 195 in the upper reaches of the Iwaidani gully, Mt. Funabuseyama area. The base map of Figure 1.2 after Sano *et al*. (1992).

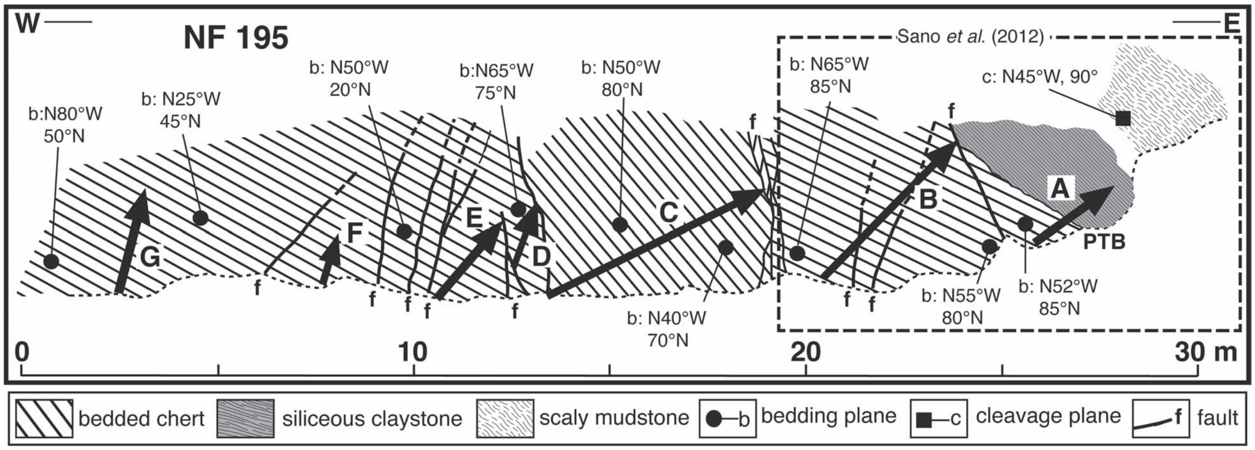

Figure 2. Field sketch showing the location of measured subsections NF195G to C, indicated by arrows, along the entire exposure of section NF 195. The stratigraphy and age of subsections NF195A and B, including the Permian-Triassic boundary, have been reported by Sano *et al*. (2012).

to NF 195C with one another by tracing individual beds in the field.

The measured subsections entirely comprise thin, ribbon-bedded chert alternating with clayey partings (Figures 3.1–3.3) and in places contain thicker intercalations of claystone, attaining a few centimeters thickness. Chert is dominantly gray. Dark gray to black chert with black and carbonaceous, clayey partings intermittently occurs at several levels (Figure 3.2). Chert of subsections NF 195G, NF 195F, and NF 195E is slightly greenish gray, alternating with slightly tuffaceous, pale green clayey partings (Figure 3.1). Ranging from 2 to 15 cm, the thickness of individual chert beds is most commonly 5 to 8 cm throughout the subsections NF 195C to NF 195G (Fig-

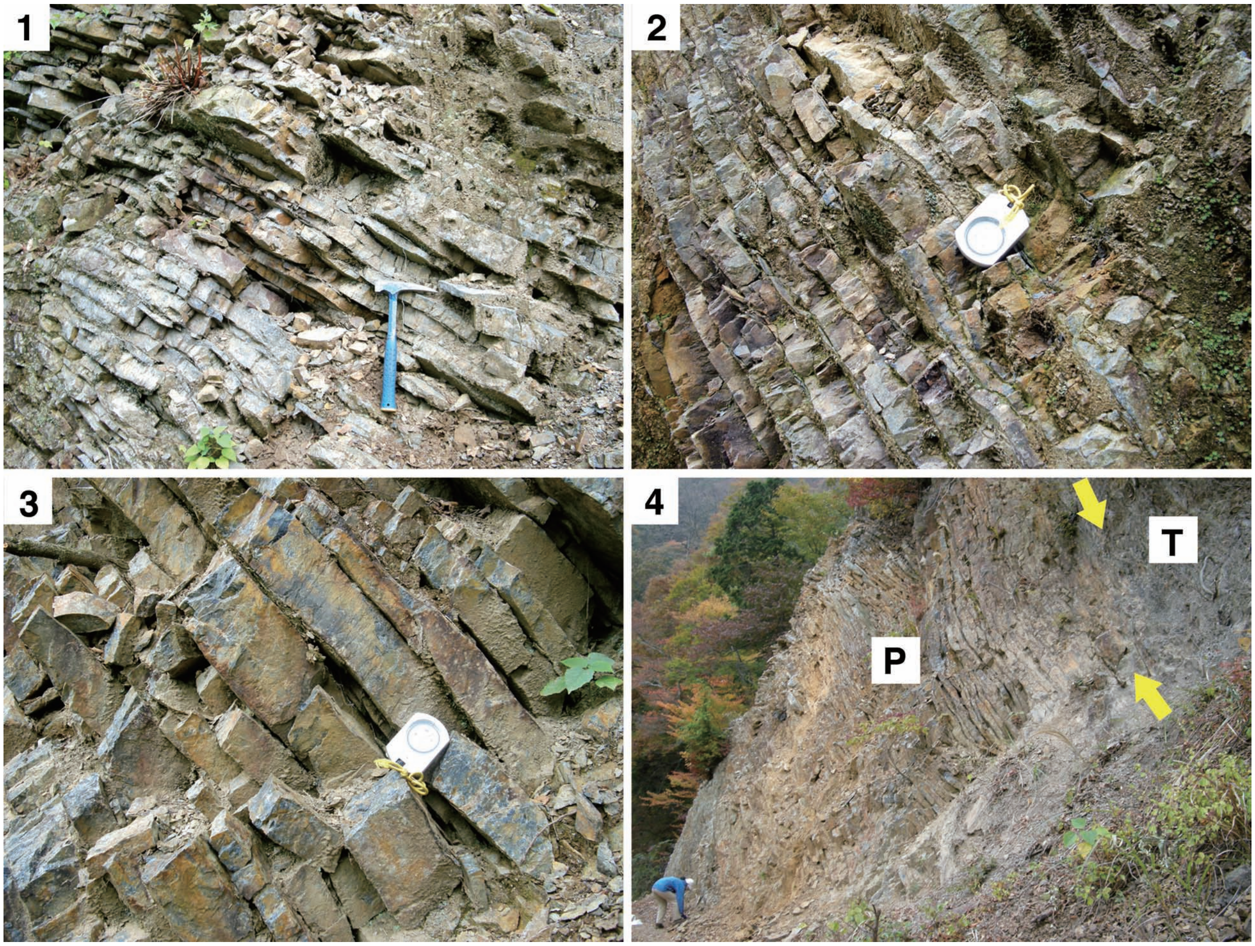

Figure 3. Photos of the bedded chert and associated black claystone of section NF 195. **1,** greenish gray chert with pale green clayey partings in the middle part of subsection NF 195G; **2,** intercalation of black chert in the upper part of subsection NF 195D; **3,** gray chert with extremely thin partings in the middle part of subsection NF 195C; **4,** oblique view of the upper part of section NF 195, comprising the upper Lopingian chert (P) and *Hindeodus parvus*-bearing lower Lower Triassic black claystone (T). Arrows indicate the position between these two lithologic units.

ures 3.1, 3.2). The thickness of chert beds tends to thicken up-section (Figure 3.3). The thickness of the clayey partings exhibits no marked stratigraphic change. The clayey partings are most usually 0.5 to 1 cm in thickness (Figures 3.1, 3.2). However, the partings in the upper part of section NF 195 (e.g., subsection NF 195C) are paper-thin, rarely exceeding a few millimeters (Figure 3.3).

Published biostratigraphic studies date the whole of section NF 195 as the upper Guadalupian to the lower Lower Triassic on the basis of the occurrence of *Albaillella triangularis* and *A. levis* (Sano, 1988a), *Neogondolella wilcoxi* (Kitao, 1996), *Follicucullus porrectus*, *A. excelsa*, and *A. triangularis* (Kuwahara, 1997), and *A. triangularis*, *Neoalbaillella optima*, and *Hindeodus parvus* (Sano *et al*., 2012). Our present biostratigraphic study showed that the beds of section NF 195 face northeast. Sano *et al*. (2012) reported that the Permian-Triassic boundary is placed at the marked lithologic boundary between the Wuchiapingian to the Changhsingian chert and overlying lower Induan black claystone (subsections NF 195A and 195B in Figure 2) in the upper part of section NF 195 (Figure 3.4).

Material and methods

We collected samples from each chert bed in subsections NF 195G to NF 195C for the radiolarian biostratigraphy. Thick beds, exceeding 15 cm, were divided into a few subsamples.

We processed a total of 262 samples of chert. The chert samples were processed using 5% HF solution for 24 hours. The residue was sieved and collected using standard sieves of 35 mesh and 200 mesh (openings 425 μm and 75 μm). One to several smear slides on which dried residue was glued with "Entellan neu" were prepared for each sample. Microscopic observations were made mainly under transmitted light, and *ca.* 2800 photomicrographs were taken.

Stratigraphic distribution of radiolarians in subsections

Identified from these subsections are 47 genera and 84 species of radiolarians. The identified radiolarians comprise eight species of four genera of Albaillellaria, 48 species and 22 genera of Latentifistularia, 15 species of nine genera of Entactinaria, and 13 species and 12 genera of Spumellaria. So far as examined, non-albaillellarian taxa greatly dominate in the number of genera and species relative to the albaillellarians.

More than 10 radiolarian species in our study do not match the descriptions or images of published species. We do not rule out the possibility that these species are new species. However, careful examination of a greater number of specimens for each of these taxa will be necessary before we can verify whether they are indeed new species. By this reason we classify and report these undesignated taxa in open nomenclature using alphabetic codes, A, B, C, etc. Brief notes on their morphologic characteristics are provided at the end of this paper.

Subsection NF 195G

Occupying the lowermost part of section NF 195, subsection NF 195G reaches *ca.* 3.45 m in thickness (Figure 4). Its succession is much dominated by gray to greenish gray chert (Figure 3.1) with intercalations of dark gray to black chert beds in the middle part (Figure 5).

Seventy-seven samples of chert from this subsection were processed (Figure 5). The preservation of radiolarian fossils is moderate in this subsection. Non-albaillellarian fossils are markedly dominant over the albaillellarians in this subsection (Figure 5). The latentifistularians are most abundant and diverse in the non-albaillellarians. We identified 25 species of 18 genera of the latentifistularians. The albaillellarians are much scarce and less diverse throughout this subsection. Their occurrence is nearly limited to the lowermost part of this subsection.

The bottom of subsection NF 195G contains abundant *Follicucullus charveti* (Figure 6.6) and *Follicucullus* spp. with a small amount of *F. bipartitus* (Figure 6.7). One specimen of *Pseudoalbaillella* sp. occurs from the basal level (Figure 5).

The lower part of this subsection (NF 195 samples 352 to 327 in Figure 5) is characterized by *Foremanhelena triangula* (Figure 7.18) and yields *Follicucullus porrectus* (Figure 6.5) and *Follicucullus*? sp. It is noted that *F. triangula* occurs in a well defined stratigraphic range from NF 195-352 to 315 (Figure 5).

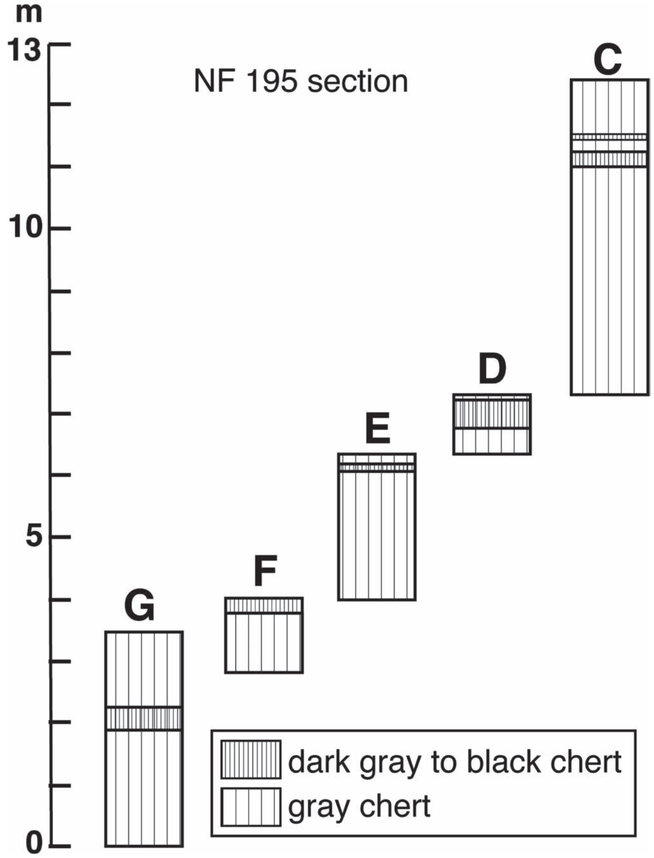

Figure 4. Lithostratigraphy of subsections NF 195G to NF 195C mainly comprising gray chert with minor dark gray to black chert. The locations of the subsections are shown in Figure 2.

Prolific occurrence of diverse latentifistularians characterizes the middle to upper part of this subsection (Figure 5). The middle part is characterized by the occurrence of *Nazarovispongus inflatum* (Figure 7.15) and *Ruzhencevispongus* sp. B (Figures 7.9, 7.10), and *Rectotormentum wardlawi* (Figure 7.3) at many levels. The upper part is marked by the occurrence of *Ruzhencevispongus* sp. C (Figures 7.11, 7.12). Other characteristic latentifistularians include *Quadricaulis inflata*, *Raciditor scalae*, *Ruzhencevispongus* spp., *Raciditor gracilis*, and *Quadrilobata*? *blomei* (Figure 7.6). Along with the latentifistularians, *Albaillella* sp. G occurs in two levels in the middle and upper parts of this subsection. *Stigmosphaerostylus* spp., *Copicyntra* spp., *Copiellintra* spp., and *Hegleria* spp. occur throughout the subsection (Figure 5).

Subsection NF 195F

Subsection NF 195F occupies the lower part of sec-

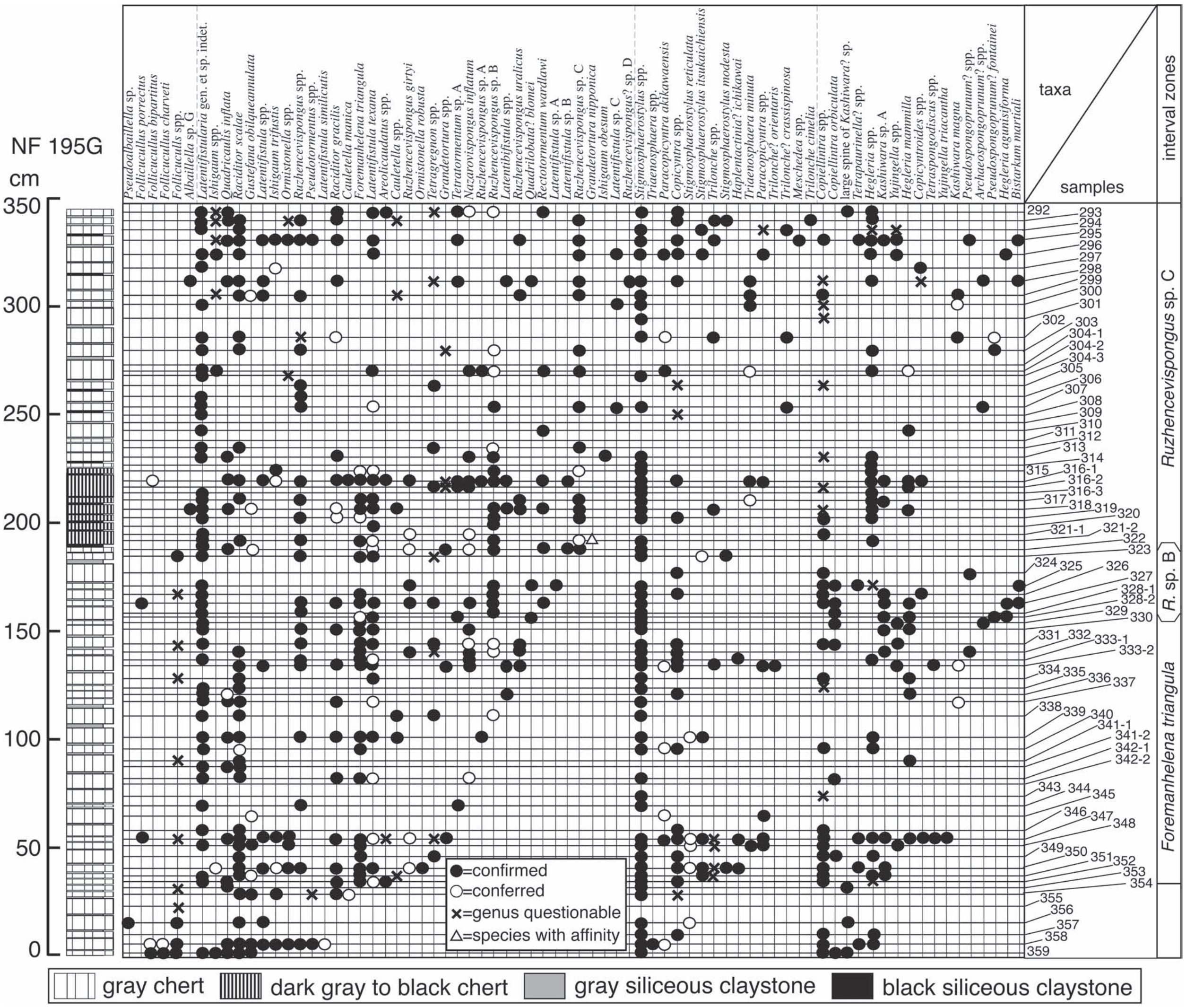

Figure 5. Stratigraphic distribution of the radiolarians in subsection NF 195G. See Figure 2 for the location in NF 195. The stratigraphic position of this subsection is shown in Figure 4.

tion NF 195 and nearly corresponds to the upper part of subsection NF 195G (Figure 4). The thickness of this subsection is 1.2 m. Its succession dominantly comprises slightly greenish gray chert and contains black chert beds with black claystone in an approximately 20-cm-thick stratigraphic interval at the top and gray siliceous claystone at a few stratigraphic levels (Figure 8).

We processed 23 samples of chert from this subsection. Radiolarian fossils in this subsection are moderately preserved. Whereas the albaillellarians are scarce, the latentifistularians are diverse and dominant in this subsection (Figure 8). The entactinarians and spumellarians also occur throughout subsection NF 195F.

The most characteristic latentifistularian species of this subsection is *Ruzhencevispongus* sp. C, which occurs at nearly all the stratigraphic levels of this subsection (Figure 8). *Nazarovispongus inflatum* is recognized at only a few levels in the lower to middle part, though widespread in the underlying subsection NF 195G. *Ruzhencevispongus* sp. B, which characterizes the middle part of subsection NF 195G, much declines in this subsection.

Non-albaillellarian species common in this subsection include *Quadricaulis inflata*, *Ruzhencevispongus* spp., *Latentifistula texana* (Figure 7.1), *Latentifistula* spp., *Raciditor gracilis*, *R. scalae*, *Ishigaum trifustis*, *Stigmosphaerostylus* spp., *Copicyntra* spp., *Copiellintra* spp., and *Hegleria* spp. (Figure 8). *Copicyntra* spp. occurs in the middle to upper part of subsection NF 195F.

Albaillellarians in subsection NF 195F are sparse and very low in diversity and include only *Albaillella* sp. G

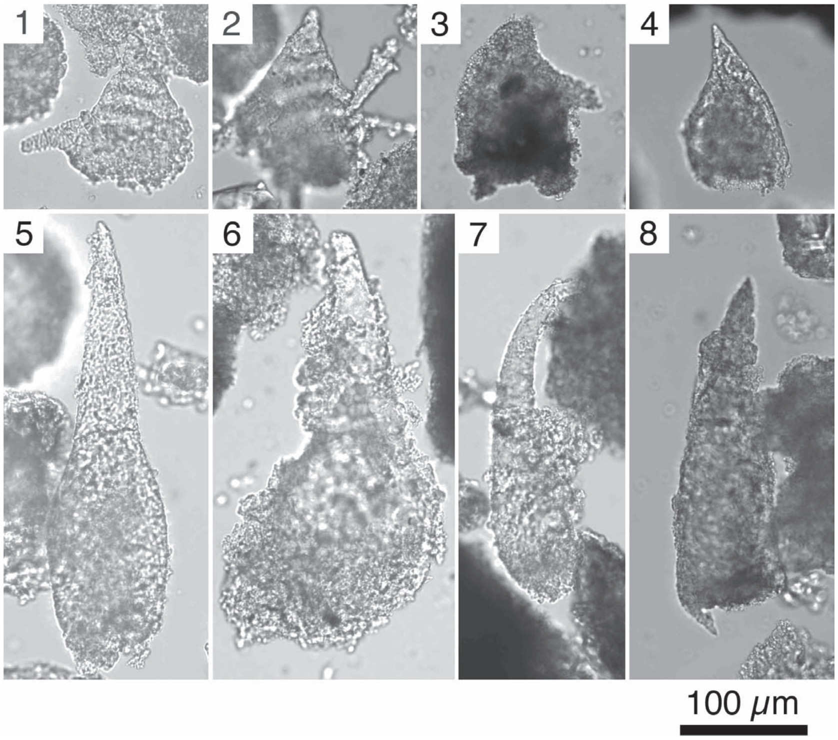

Figure 6. Photomicrographs of representative albaillellarian fossils from subsections NF 195G to NF 195C. See Figures 5 and 8 to 11 for the stratigraphic positions of the samples. Scale bar represents 100 µm. Transmitted light. **1,** *Albaillella* sp. G, NF 195-298; **2,** *Albaillella yamakitai* Kuwahara, NF 195-263; **3,** *Albaillella cavitata* Kuwahara, NF 195-207; **4,** *Albaillella protolevis* Kuwahara, NF 195-143; **5,** *Follicucullus porrectus* Rudenko, NF195-327; **6,** *Follicucullus charveti* Caridroit and De Wever, NF 195-359; **7,** *Follicucullus bipartitus* Caridroit and De Wever, NF 195-359; **8,** *Follicucullus* sp., NF 195-209.

and *Follicucullus* sp. at a few levels (Figure 8). *Albaillella* sp. G is poorly preserved and occurs scattered in the lower and upper parts of this subsection. Even the identification at the genus level for *Follicucullus.* sp. is questionable, for it is also badly preserved and occurs at only one level in the lower part of this subsection (Figure 8).

Subsection NF 195E

Subsection NF 195E lies in the lower part of section NF 195 (Figure 4). We correlated the bottom of this subsection and the top of subsection NF 195F by tracing individual beds in the field. Though separated by faults (Figure 2), these two subsections are definitely successive. Subsection NF 195E attains approximately 2.4 m in thickness (Figure 9). Its succession consists dominantly of the gray bedded chert. A minor amount of the dark gray to black chert occurs intercalated in the upper part.

We processed 54 samples of chert from this subsection (Figure 9). The preservation of radiolarians in this subsection is moderate. This subsection bears highly diverse latentifistularians (Figure 9). We identified 20 genera and 34 species of Latentifistularia, which is most diverse among the radiolarians in this subsection. Latentifistularians occur throughout this subsection, markedly in its lower to middle part (Figure 9). Occurring scattered in this subsection, the albaillellarians are much less diverse than the non-albaillellarians.

Though intermittently, *Triplanospongos angustus* (Figure 7.19) occurs throughout this subsection (Figure 9). *Latentifistula* sp. B is yielded at many levels of this subsection. *Ruzhencevispongus* sp. C having a triangular shape characterizes the lower to middle part of this subsection (Figure 9). Its lower part yields *Tetratormentum* sp. A (Figure 7.4), *Triplanospongos* sp. B (Figure 7.5), *R. girtyi*, *R. uralicus*, *R. rotundus*, *Ruzhencevispongus* sp. A (Figures 7.7, 7.8), *Ruzhencevispongus* sp. B, and *Ruzhencevispongus* sp. D (Figures 7.13, 7.14).

Albaillella yamakitai (Figure 6.2) occurs in the lower and upper parts of this subsection (Figure 9). The genus *Follicucullus*, including *F. porrectus*, *F. charveti*, and *Follicucullus* spp., sporadically occurs in the lower to middle part.

Subsection NF 195D

Subsection NF 195D lies in the lower part of section NF 195 (Figure 4). Though both the bottom and top of

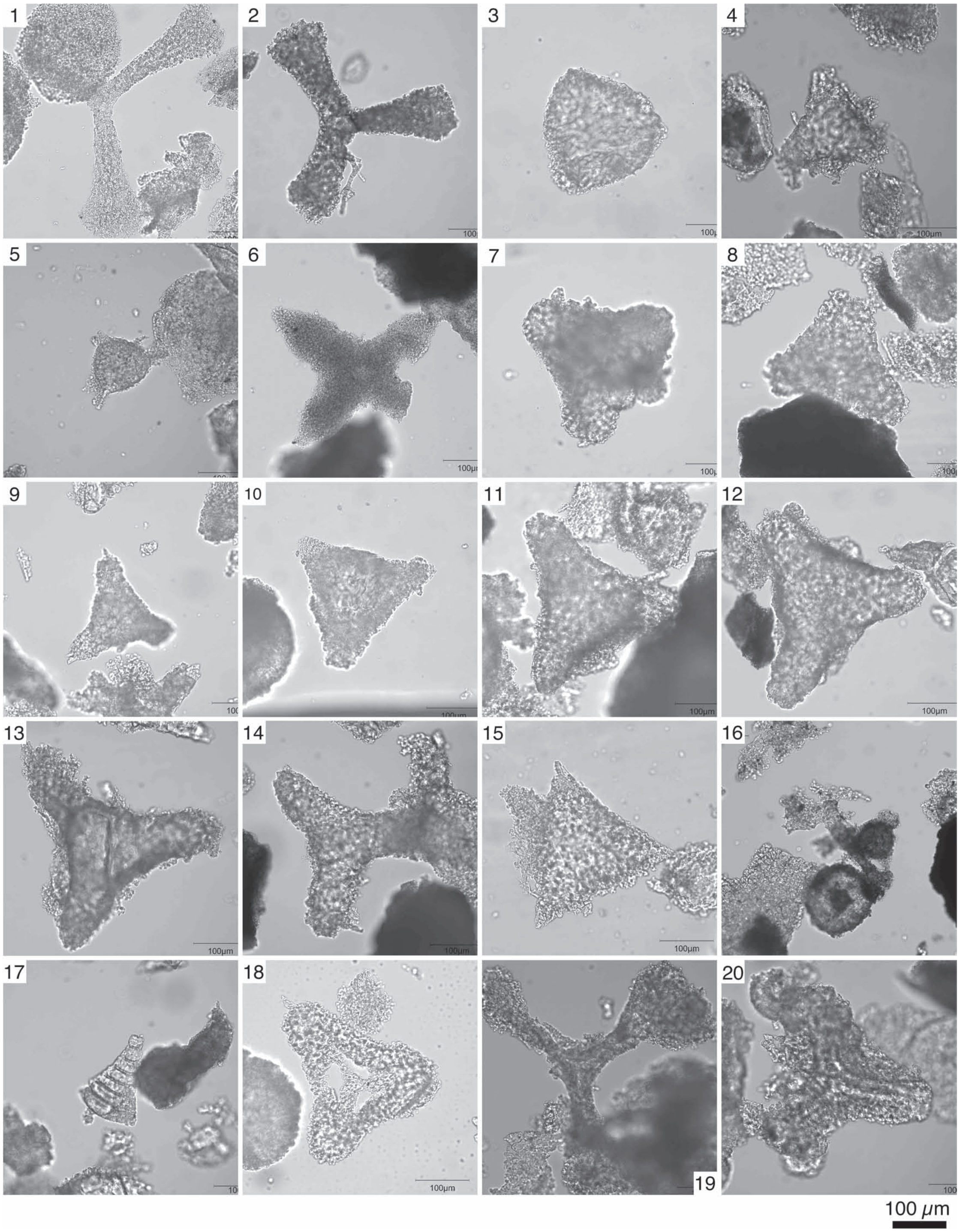

Figure 7. Photomicrographs of representative latentifistularian fossils from subsections NF 195G to NF 195C. See Figures 5 and 8 to 11 for the stratigraphic positions of the samples. Scale bar represents 100 μm. Transmitted light. **1,** *Latentifistula texana* Nazarov and Ormiston, NF 195-285-2; **2,** *Latentibifistula asperspongiosa* Sashida and Tonishi, NF 195-141; **3,** *Rectotormentum wardlawi* Nestell and Nestell, NF 195-318; **4,** *Tetratormentum* sp. A, NF 195-269; **5,** *Tetratormentum* sp. B, NF 195-270; **6,** *Quadrilobata*? *blomei* Nestell and Nestell, NF 195-224; **7,** *Ruzhencevispongus* sp. A, NF 195-304-2; **8,** *Ruzhencevispongus* sp. A, NF 195-339; **9,** *Ruzhencevispongus* sp. B, NF 195-316-1; **10,** *Ruzhencevispongus* sp. B, NF 195-326; **11,** *Ruzhencevispongus* sp. C, NF 195-296; **12,** *Ruzhencevispongus* sp. C, NF 195-304-2; **13,** *Ruzhencevispongus*? sp. D, NF 195-265; **14,** *Ruzhencevispongus*? sp. D, NF 195-266; **15,** *Nazarovispongus inflatum* (Nazarov and Ormiston), NF 195-330; **16,** *Cauletella paradoxa* Shang, Caridroit, and Wang, NF 195-208-1; **17,** *Cauletella porosa* Feng, NF 195-136; **18,** *Foremanhelena triangula* De Wever and Caridroit, NF 195-333-2; **19,** *Triplanospongos angustus* (Noble and Renne), NF 195-255; **20,** *Triplanospongos musashiensis* Sashida and Tonishi, NF 195-126.

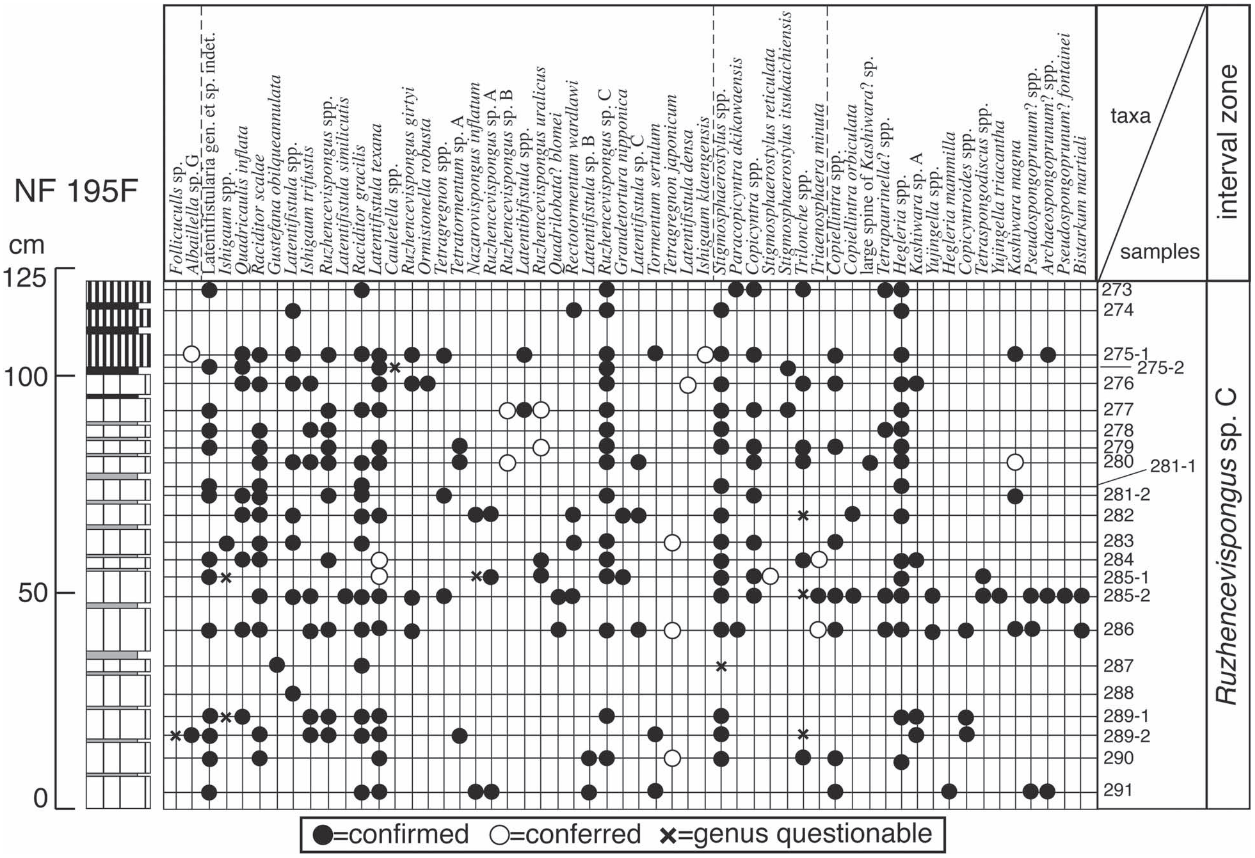

Figure 8. Stratigraphic distribution of the radiolarians in subsection NF 195F. See Figure 2 for the location in NF 195. The stratigraphic position of this subsection is shown in Figure 4. See Figure 5 for the lithologic symbols.

this subsection are bounded by steeply inclined faults (Figure 2), we confirmed the stratigraphically continuous relation of this subsection to its under- and overlying subsections in the field.

This subsection (~1 m in thickness) comprises gray chert in the lower part and dark gray to black chert in the upper part (Figure 10). The gray chert beds alternate with gray siliceous claystone partings, slightly thicker than usual, and the dark gray to black chert beds have black claystone partings (Figure 10). In total 19 chert samples from this subsection were processed. Although the extracted radiolarian fossils are poorly preserved, they include 7 species of 3 genera of Albaillellaria, 26 species of 16 genera of Latentifistularia, 10 species of 6 genera of Entactinaria, and 12 species of 9 genera of Spumellaria (Figure 10).

Latentifistularian species widespread in this subsection are *Quadricaulis inflata*, *Raciditor scalae*, *Gustefana obliqueannulata*, *Latentifistula texana*, and *Latentifistula* sp. B (Figure 10). *Triplanospongos* cf. *angustus*, which occurs throughout the underlying subsection NF 195E, is yielded in the middle part of this subsection as well. The middle to upper part is also characterized by the occurrence of *Albaillella cavitata* (Figure 6.3) along with *A. protolevis* at the topmost level. *Follicucullus porrectus* and *Follicucullus* sp. (Figure 6.8) are extracted from the upper part of the subsection. *Cauletella paradoxa* occurs in the upper part. *Stigmosphaerostylus* spp. and *Hegleria* spp. yield throughout this subsection.

Subsection NF 195C

Subsection NF 195C is in the middle part of section NF 195 (Figure 4). The thickness of this subsection is up to 5.1 m. Although the base of the section is cut by a nearly vertical fault (Figure 2), we confirmed its stratigraphic continuity with the underlying subsection NF 195D by tracing of the individual beds in the field.

This subsection chiefly comprises gray chert with intermittent intercalations of dark gray to black chert and relatively thick beds of gray siliceous claystone (Figure 11). Clayey partings are occasionally paper-thin in the middle part (Figure 3.3). Highly carbonaceous black claystone

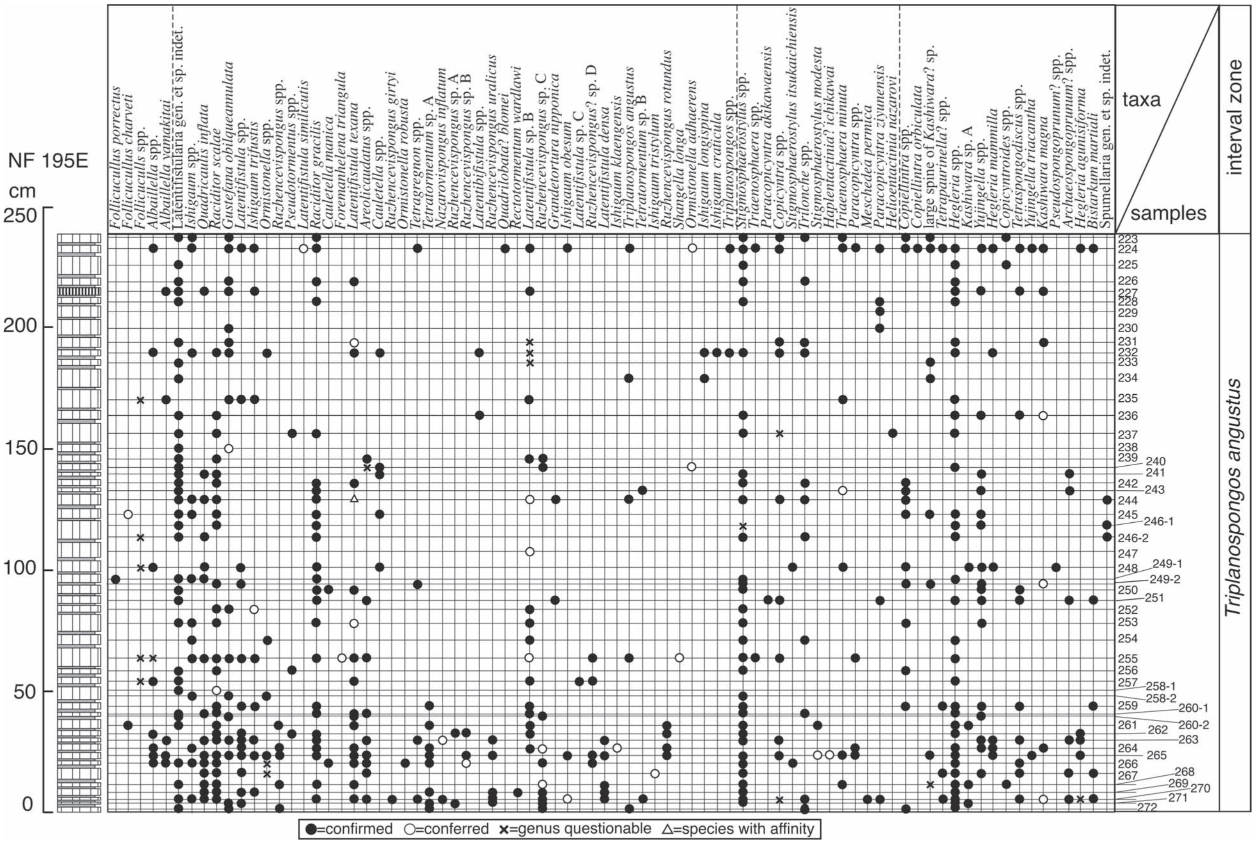

Figure 9. Stratigraphic distribution of the radiolarians in subsection NF 195E. See Figure 2 for the location in NF 195. The stratigraphic position of this subsection is shown in Figure 4. See Figure 5 for the lithologic symbols.

partings are associated with the dark gray to black chert.

Diverse radiolarians were extracted from a total of 89 samples of chert from this subsection (Figure 11). The extracted radiolarians include 3 species of 3 genera of Albaillellaria, 34 species of 19 genera of Latentifistularia, 13 species of 8 genera of Entactinaria, and 11 species representing 11 genera of Spumellaria. Most of the extracted radiolarian specimens are poorly preserved.

The latentifistularian species occur throughout the subsection NF 195C (Figure 11). The lower part of this subsection yields *Latentifistula* sp. B, *Latentifistula* spp., and *Raciditor scalae*. The upper part of the subsection is characterized by the abundant occurrence of *Cauletella porosa* (Figure 7.17), *Triplanospongos musashiensis* (Figure 7.20), and *Latentibifistula asperispongiosa* (Figure 7.2). *T. angustus* and *C. paradoxa* (Figure 7.16) occur throughout the subsection. *Kashiwara magna* is yielded throughout this subsection (Figure 11), but its upper part records the acme of this species.

Albaillellarians are sparse in the lower to middle part of this subsection and abundant in its upper part (Figure 11). The occurrence of the genus *Follicucullus* is limited to the lower part; *F. porrectus* from NF 195-184 and *Follicucullus*? sp. from NF195-186. In the upper part of this subsection, *Albaillella protolevis* (Figure 6.4) continuously occurs in the interval from NF195-148 to NF195-125 and *Neoalbaillella pseudogrypa* is borne sporadically at the three levels in the upper part (Figure 11).

Brief notes on species left in open nomenclature

So far as surveyed, 16 species of the radiolarians do not match any published species. Those left in open nomenclature using alphabetic designations are *Albaillella* sp. G (Figure 6.1), *Latentibifistula* sp. A, *Latentifistula* sp. A, *Latentifistula* sp. B, *Latentifistula* sp. C, *Ormistonella* sp. A, *Ruzhencevispongus* sp. A (Figures 7.7, 7.8), *Ruzhencevispongus* sp. B (Figures 7.9, 7.10), *Ruzhencevispongus* sp. C (Figures 7.11, 7.12), *Ruzhencevispongus* sp. D (Figures 7.13, 7.14), *Tetratormentum* sp. A (Figure 7.4), *Tetratormentum* sp. B (Figure 7.5), *Kashiwara* sp. A, Latentifistularia gen. et sp. indet. A, Spumellaria gen. et sp. indet. A, and Spumellaria gen. et sp. indet. B. Brief notes on the characteristics of the following seven species important for establishing the interval zones are

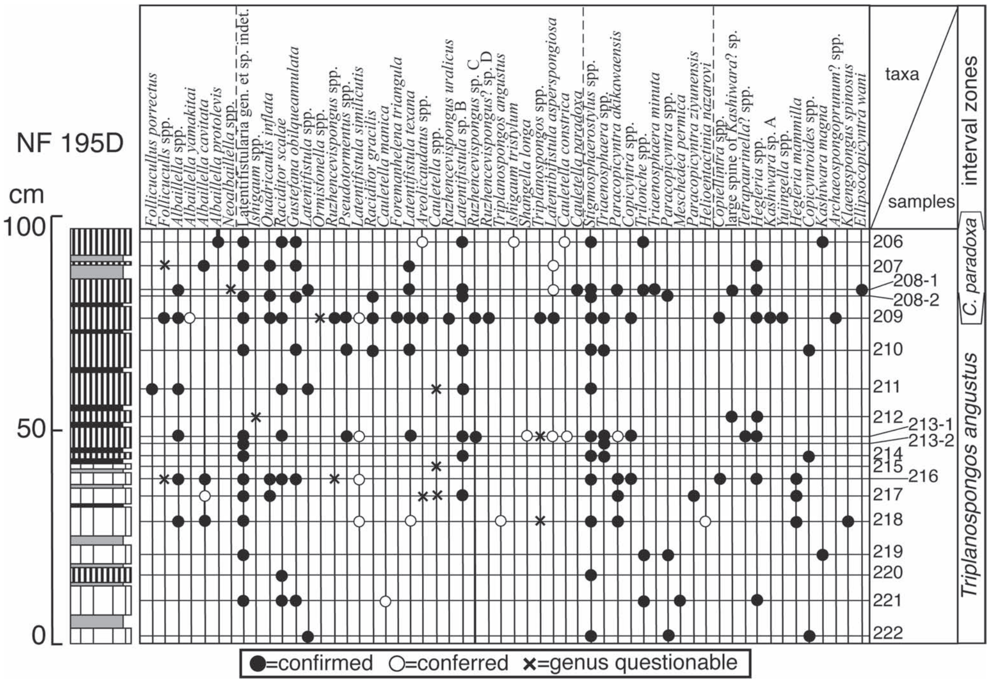

Figure 10. Stratigraphic distribution of the radiolarians in subsection NF 195D. See Figure 2 for the location in NF 195. The stratigraphic position of this subsection is shown in Figure 4. See Figure 5 for the lithologic symbols.

given below.

Albaillella sp. G (Figure 6.1) is identical with *Albaillella* sp. G of Kuwahara (1999), whereas some paleontologists in North America and China consider this species as a variety of *A. yamakitai* (e.g. Xia *et al*., 2005; Maldonado and Noble, 2010). *Albaillella yamakitai* has a ventral wing that occurs between the third and forth transverse bands in the original description (Kuwahara, 1999), while the ventral wing of *Albaillella* sp. G protrudes from near the last transverse band. Therefore we discriminate *Albaillella* sp. G from *A. yamakitai* by the position of the protruding wing.

Ruzhencevispongus sp. A (Figures 7.7, 7.8) has a platy and inflated shape having a triangular outline with rounded ends, and is similar to *R. uralicus* of Kozur (1980). However, as *Ruzhencevispongus* sp. A is larger than *R. uralicus* in size and characteristically has rounded ends, we differentiate *Ruzhencevispongus* sp. A from *R. uralicus*.

Ruzhencevispongus sp. B (Figures 7.9, 7.10) is small in size. It is similar in having a platy and inflated shape with three arms, but its central part is markedly inflated. The three arms of *Ruzhencevispongus* sp. B are short and slightly knobby in their distal ends.

Ruzhencevispongus sp. C (Figures 7.11, 7.12) is robust and large, characterized by a platy and triangular shape with a inflated central part and three long and thick arms with rounded ends. *Ruzhencevispongus* sp. C and *Ruzhencevispongus*? sp. D (Figures 7.13, 7.14) are similar in shape to each other, but the latter is discriminated from the former by having longer and slender arms.

Tetratormentum sp. A (Figure 7.4) is characterized by having a tetrahedral shape with four arms. *Tetratormentum* sp. B (Figure 7.5) is similar in having a tetrahedral shape to *Tetratormentum* sp. A, but is smaller than *Tetratormentum* sp. A. *Tetratormentum* sp. B is also differentiated from *Tetratormentum* sp. A by having short, rod-shaped spines extruding from the ends of the arms. Each side of the tetrahedral shell of *Tetratormentum* sp. A is concave, while that of *Tetratormentum* sp. B is convex.

Late Guadalupian to early Lopingian radiolarian interval zones

Focusing on the first appearance datum (FAD) of the latentifistularians, we propose six late Guadalupian (late Capitanian) to early Lopingian (early Wuchiapingian) Latentifistularia-based interval zones. They are the (1) *Foremanhelena triangula* Interval Zone, (2) *Ruzhencevispongus* sp. B Interval Zone, (3) *Ruzhencevispongus* sp. C Interval Zone, (4) *Triplanospongos angustus* Interval Zone, (5) *Cauletella paradoxa* Interval Zone, and (6) *Triplanospongos musashiensis* Interval Zone, in ascending order (Figure 12). We herein provide their defini-

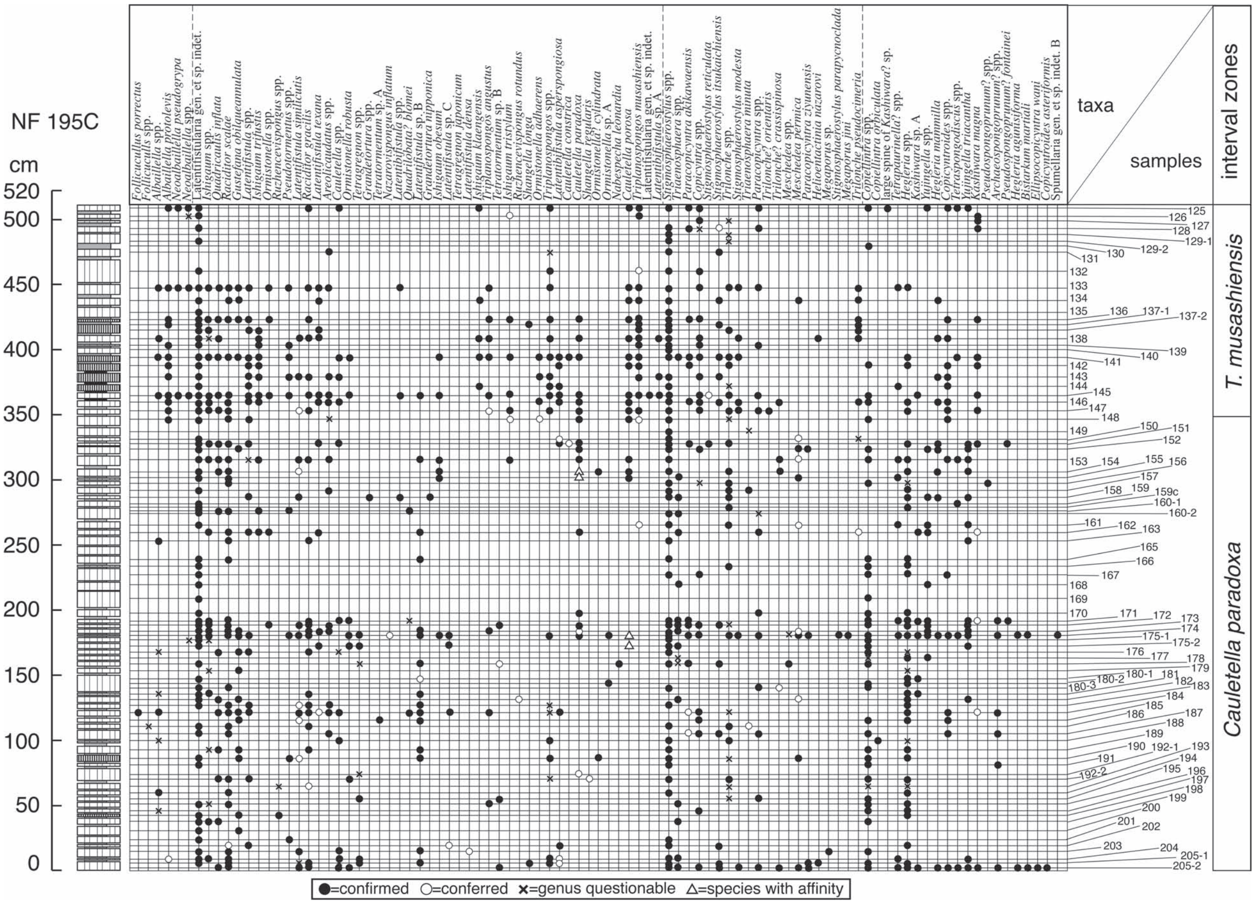

Figure 11. Stratigraphic distribution of the radiolarians in subsection NF 195C. See Figure 2 for the location in NF 195. The stratigraphic position of this subsection is shown in Figure 4. See Figure 5 for the lithologic symbols.

tion, stratigraphic distribution, age, and biostratigraphic remarks.

Foremanhelena triangula Interval Zone

Definition.—The base of this interval zone is defined by FAD of *Foremanhelena triangula* (NF 195-352 in Figures 5, 12). The top of this zone is defined by FAD of *Ruzhencevispongus* sp. B (NF 195-328-1).

Stratigraphic Distribution.—This interval zone corresponds to the 126-cm-thick succession mainly of the gray chert in the lower part of subsection NF195G (Figure 12). This zone is underlain by an unnamed biozone in the basal part of subsection NF 195G. The unnamed zone bears *Follicucullus charveti* and *Follicucullus* spp. with minor amounts of *F. bipartitus* and *Pseudoalbaillella* sp. (Figure 5).

Age.—late Capitanian.

Remarks.—*Foremanhelena triangula* is abundant in this zone. Common species are *Raciditor scalae*, *R. gracilis and Latentifistula texana*. *Nazarovispongus inflatum* occurs in the upper part of this zone. *Follicucullus porrectus* and *Follicucullus*? sp. are rare and co-occur with these latentifistularians.

Ruzhencevispongus sp. B Interval Zone

Definition.—The base of this interval zone is defined by FAD of *Ruzhencevispongus* sp. B (NF 195-328-1 in Figures 5, 12). FAD of *Ruzhencevispongus* sp. C. defines the top of this zone (NF 195-322).

Stratigraphic distribution.—The 30-cm-thick succession of gray chert in the middle part of subsection NF 195G corresponds with this interval zone (Figure 12).

Age.—late Capitanian.

Remarks.—*Foremanhelena triangula* and *Ruzhencevispongus* sp. B are abundant in this zone. *Latentifistula texana* is also common. *Follicucullus porrectus* and *Follicucullus*? sp. are rare and co-occur with these latentifistularians.

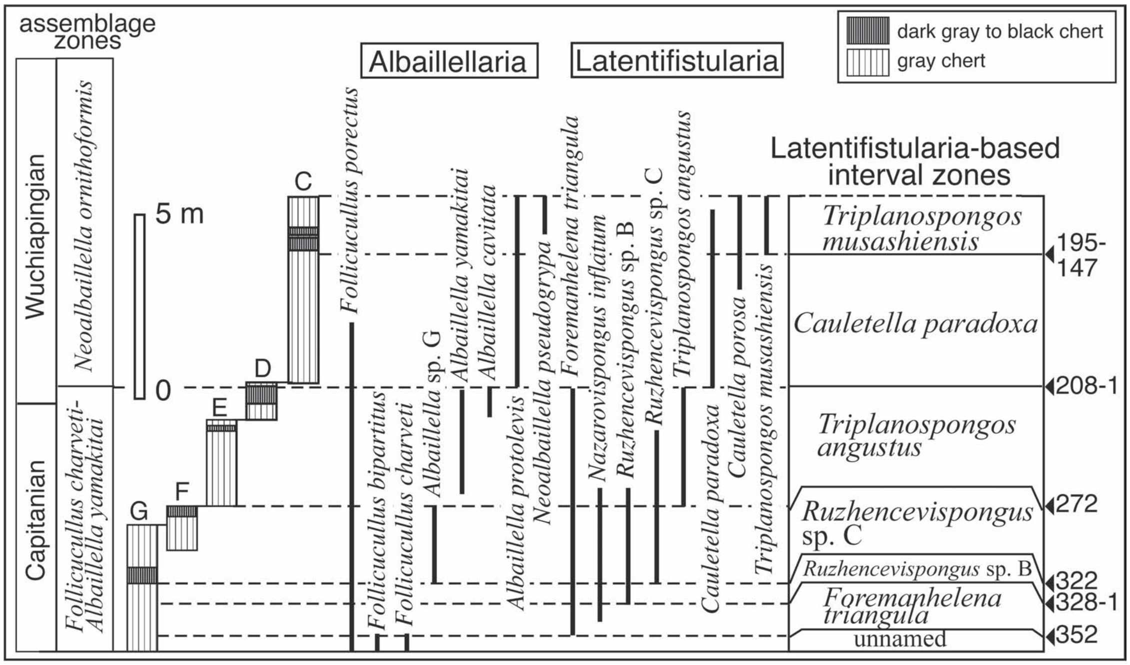

Figure 12. Upper Capitanian to lower to middle (?) Wuchiapingian Latentifistularia-based interval zones in subsections NF 195 G to C, and their correlation to Albaillellaria-based assemblage zones (Kuwahara *et al*., 1998, emended by Kuwahara, 1999). Sample numbers at the right margin correspond with boundary levels of each interval zone.

Ruzhencevispongus sp. C Interval Zone

Definition.—The base of this interval zone is defined by FAD of *Ruzhencevispongus* sp. C (NF 195-322 in Figures 5, 12). FAD of *Triplanospongos angustus* defines the top of this zone (NF 195-272 in Figure 9).

Stratigraphic distribution.—Approximately 160-cm-thick dark gray to black and gray chert succession in the upper part of subsection NF195G and 120-cm-succession of the gray chert from NF195-291 to NF195-273 of subsection NF 195F correspond to this interval zone (Figure 12).

Age.—late Capitanian.

Remarks.—*Foremanhelena triangula* is abundant in the lowermost part of this zone. *Ruzhencevispongus* sp. B occurs at many levels in the lower part of this zone, closely corresponding with the lower part of subsection NF 195G (Figures 5, 12). *Nazarovispongus inflatum* is found sporadically in this zone. Common species in this zone are *Quadricaulis inflata, Raciditor scalae, R. gracilis, Latentifistula texana* and *Latentifistula* spp., and *Albaillella* sp. G is rare.

Triplanospongos angustus Interval Zone

Definition.—FAD of *Triplanospongos angustus* defines the base of this interval zone (NF 195-272 in Figures 9, 12). Its top is defined by FAD of *Cauletella paradoxa* (NF 208-1 in Figure 10)

Stratigraphic distribution.—Approximately 240-cm-thick chert succession from NF195-272 to NF195-223 comprising the entirety of subsection NF195E plus 90-cm-thick chert succession from NF195-222 to NF195-209 of subsection NF195D correspond to this interval zone (Figure 12).

Age.—late Capitanian to early Wuchiapingian.

Remarks.—*Albaillella yamakitai* and *A. cavitata* occur scattered in this zone. The occurrence of *Ruzhencevispongus* sp. C, nominal species of the underlying interval zone, extends into this interval zone. *Triplanospongos angustus* is yielded throughout subsection E (Figure 9), but occurs at only one level in the lower part of subsection D (Figure 10).

Cauletella paradoxa Interval Zone

Definition.—FAD of *Cauletella paradoxa* defines the base of this interval (NF 195-208-1 in Figures 10, 12). Its top is defined by FAD of *Triplanospongos musashiensis* (NF 195-147 in Figure 11).

Stratigraphic distribution.—This biozone corresponds with the topmost 15-cm-thick succession comprising the black chert of subsection D (NF195-208-1 to NF195-206 in Figure 12) plus the 350-cm-thik succession of the gray chert in the lower to middle part of subsection C (NF195-205-2 to NF195-148).

Age.—early Wuchiapingian.

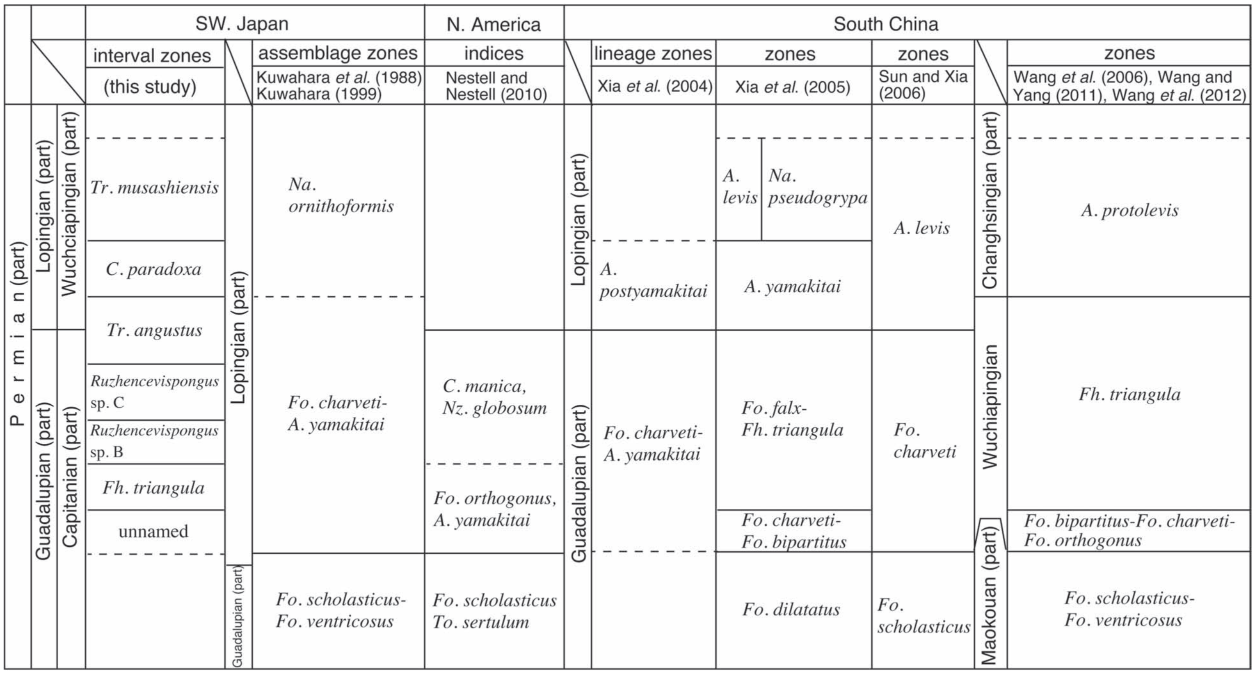

Figure 13. Stratigraphic comparison of the newly proposed upper Capitanian to lower Wuchiapingian Latentifistularia-based interval zones (this study) with Albaillellaria-based assemblage zones (Kuwahara *et al*., 1998, emended by Kuwahara, 1999) in Japan, radiolarian indices in North America (Nestell and Nestell, 2010), and radiolarian zones in South China (Xia *et al*., 2004, 2005; Sun and Xia, 2006; Wang *et al*., 2006; Wang and Yang, 2011; Wang *et al*., 2012). *A.*: *Albaillella*; *C.*: *Cauletella*; *Fo.*: *Follicucullus*; *Fh.*: *Foremanhelena*; *Na.*: *Neoalbaillella*; *Nz.*: *Nazarovispongus*; *To.*: *Tormentum*; *Tr.*: *Triplanospongos*.

Remarks.—*Albaillella cavitata* occurs in the lowermost part of this zone. *Albaillella protolevis* and *Albaillella* sp. occurs sporadically in this zone. *Cauletella porosa* appears in the uppermost part of this interval zone.

Triplanospongos musashiensis Interval Zone

Definition.—FAD of *Triplanospongos musashiensis* defines the base of this interval zone (NF 195-147 in Figures 11, 12). Its top remains undefined.

Stratigraphic distribution.—The approximately 1.6-m-thick succession in the upper part of subsection NF 195C, composed of dark gray to black chert in the lower and gray chert in the upper, is assigned to this interval zone.

Age.—Early to middle (?) Wuchiapingian.

Remarks.—This interval zone yields *Neoalbaillella pseudogrypa*, *Albaillella protolevis*, *Triplanospongos angustus*, *Cauletella paradoxa*, and *C. porosa*.

Triplanospongos musashiensis is reported to occur from the Asselian to Sakmarian chert in eastern Thailand (Saesaengseerung *et al*., 2009), much earlier than in the Mt. Funabuseyama area. We think a further study could figure out the correct stratigraphic range of *Triplanospongos musashiensis*.

Correlation of proposed interval zones with published biozones

Correlation with Japanese assemblage zones

Kuwahara *et al*. (1998) established the following upper Guadalupian to lower Lopingian radiolarian assemblage zones in Japan; *Follicucullus charveti-Albaillella* sp. F and *Neoalbaillella ornithoformis* assemblage zones in ascending order. Then the former zone was re-named as the *Follicucullus charveti-Albaillella yamakitai* Assemblage Zone, because *Albaillella* sp. F was designated as a new species, *A. yamakitai*, by Kuwahara (1999).

On the basis of the stratigraphic distribution of the albaillellarians co-occurring with the latentifistularians, the *Foremanhelena triangula*, *Ruzhencevispongus* sp. B, *Ruzhencevispongus* sp. C, and *Triplanospongos angustus* interval zones in the study section are correlated with the *Follicucullus charveti-Albaillella yamakitai* Assemblage Zone (Kuwahara *et al*., 1998; emended by Kuwahara, 1999) (Figures 12, 13). The following *Cauletella paradoxa* and *Triplanospongos musashiensis* interval zones are comparable with the *Neoalbaillella ornithoformis* Assemblage Zone. Thus, the chert succession of subsections NF 195G, F, E, and D, except its uppermost part, is assigned to the *Follicucullus charveti-Albaillella yamaki-*

tai Assemblage Zone (Figure 12). The uppermost part of subsection NF 195D and the entirety of subsection NF 195C are correlated with the *Neoalbaillella ornithoformis* Assemblage Zone.

Kuwahara *et al*. (1998) correlated the *Follicucullus charveti-Albaillella yamakitai* and *Neoalbaillella ornithoformis* assemblage zones with the upper Guadalupian and lower Lopingian respectively (Figure 13). However, later studies (e.g. Xia *et al*., 2004; Nishikane *et al*., 2011) suggest the age assignment of these two assemblage zones by Kuwahara *et al*. (1998) should be revised.

Nishikane *et al*. (2011) examined the radiolarian and conodont biostratigraphy of the GD section of chert in the Gujo-Hachiman area, central Japan, where Kuwahara *et al*. (1998) recognized the upper Capitanian to Changhsingian radiolarian assemblage zones. The biostratigraphic study of Nishikane *et al*. (2011) much focused on the stratigraphic position of the Guadalupian-Lopingian boundary.

With an emphasis upon the stratigraphic distribution of age-diagnostic conodonts, Nishikane *et al.* (2011) proposed the "Guadalupian-Lopingian boundary transition zone" in the GD section. The transition zone is defined as a stratigraphic interval (*ca.* 1 m thick) between the levels of the first occurrence of *Clarkina postbitteri hongshuiensis* and *Clarkina postbitteri postbitteri*. On the basis of the comparison with the Chinese conodont biostratigraphy, the transition zone is thought to include the topmost of the Guadalupian and the bottom of the Lopingian (Nishikane *et al*., 2011).

Xia *et al*. (2004, 2005) defined the Guadalupian-Lopingian boundary on the basis of the first occurrence level of *Albaillella yamakitai*. However, the biostratigraphic examination of the albaillellarians in the GD section by Nishikane *et al*. (2011) shows the first occurrence of *A. yamakitai* from a few centimeters below the base of their transition zone. Thus, these authors demonstrate that the first occurrence level of *A. yamakitai* is correlated with the uppermost Capitanian.

Our radiolarian biostratigraphic examination shows the first occurrence levels of *Albaillella yamakitai* and *A. cavitata* from NF 195-266 in the lower part of subsection NF 195E and NF 195-218 in the lower part of subsection NF195D, respectively (Figures 9, 10). Following the age assignment by Nishikane *et al*. (2011), the stratigraphic interval from the lower part of subsection NF 195E to the lower part of subsection NF 195D, both corresponding with the *Triplanospongos angustus* Interval Zone, are correlated with the uppermost Capitanian (Figure 12). As *A. protolevis* and *Neoalbaillella*? sp. are extracted from the upper part of subsection NF 195D (Figure 10), it is assigned to the lower Wuchiapingian. Thus, we infer that the Guadalupian-Lopingian boundary is placed within the *Triplanospongos angustus* Interval Zone, which covers subsection NF 195E and most of subsection NF 195D (Figures 12, 13).

Correlation with Chinese radiolarian faunas and assemblage zones

Capitanian to Wuchiapingian radiolarians have been studied by several researchers in south China (e.g. Xia *et al*., 2004, 2005; Sun and Xia, 2006; Wang *et al*., 2006; Wang and Yang, 2011; Wang *et al*., 2012). Sun and Xia (2006) have shown that *Albaillella yamakitai* and *Albaillella* sp. G first appear in the middle part of the *Follicucullus charveti* Zone in the Dachongling section, Guangxi. The difference between the Dachongling section and subsections NF 195G to NF 195C is that the first occurrence of *A. yamakitai* and *Albaillella* sp. G is at the same level in the Dachongling section, while *Albaillella* sp. G appears much earlier than *A. yamakitai* in subsections NF 195G to NF 195C (Figures 5, 9). Despite the difference, the Dachongling section is basically similar with respect to the biostratigraphic succession of the major albaillellarians to subsections NF 195G to NF 195C. On the basis of the comparison we consider that the *Foremanhelena triangula*, *Ruzhencevispongus* sp. B, *Ruzhencevispongus* sp. C, and the lower part of the *Triplanospongos angustus* interval zones are correlated with the *Follicucullus charveti* Zone of Sun and Xia (2006) (Figure 13). Thus we infer that the *Cauletella paradoxa* and *Triplanospongos musashiensis* interval zones of the present study correspond with the *Albaillella levis* Zone of Sun and Xia (2006).

Sun and Xia (2006) made a correlation between the radiolarian and conodont biozones in the Dachongling section. These authors consider that their *Follicucullus charveti* and *Albaillella levis* zones are correlated with the *Clarkina postbitteri hongshuiensis* and *Clarkina postbitteri postbitteri* zones, respectively, each being correlative with the uppermost Capitanian and the lowermost Wuchiapingian. According to the correlation of the interval zones of the present study with the radiolarian zones of Sun and Xia (2006), the *Foremanhelena triangula*, *Ruzhencevispongus* sp. B, and *Ruzhencevispongus* sp. C interval zones are referred to the uppermost Capitanian (Figure 13). The *Triplanospongos angustus* Interval Zone is presumed to correlate with the topmost Capitanian to the bottom of the Wuchiapingian, ranging across the Guadalupian-Lopingian boundary.

According to the comparison by Nestell and Nestell (2010), the *Follicucullus charveti-Albaillella yamakitai* Assemblage Zone (Kuwahara *et al*., 1998; emended by Kuwahara, 1999) is correlated with the *Follicucullus charveti-Albaillella yamakitai* Zone of Xia *et al*. (2004), *Follicucullus charveti-Follicucullus bipartitus* and *Fol-*

licucullus falx-Foremanhelena triangula zones of Xia *et al*. (2005), and *Follicucullus charveti* Zone of Sun and Xia (2006). The correlation by Nestell and Nestell (2010) means that the *Foremanhelena triangula*, *Ruzhencevispongus* sp. B, *Ruzhencevispongus* sp. C, and lower part of the *Triplanospongos angustus* interval zones of the present study are correlated with the *Follicucullus charveti-Albaillella yamakitai* Zone of Xia *et al*. (2004) and *Follicucullus charveti* Zone of Sun and Xia (2006) (Figure 13). As the unnamed zone of the present study is correlated with the *Follicucullus charveti*-*Follicucullus bipartitus* Zone of Xia *et al*. (2005) (Figure 13), these four interval zones are correlated with the *Follicucullus falx-Foremanhelena triangula* Zone of Xia *et al*. (2005).

Wang and Yang (2011), Wang *et al*. (2006), and Wang *et al*. (2012) established the Permian radiolarian zones and discussed their age assignment in South China. These authors correlated both their *Follicuculls bipartitus*-*F. charveti*-*F. orthogonus* Assemblage Zone and *Foremanhelena triangula* Abundance Zone to the Wuchiapingian. The *Foremanhelena triangula* Abundance Zone could be correlated to the *Foremanhelena triangula* Interval Zone of this study.

Comparison with North American radiolarian assemblages

The Capitanian radiolarians have long been investigated chiefly in the Delaware Basin of Guadalupe Mountains, western United States since the new finding of the genus *Follicucullus* by Ormiston and Babcock (1979). Occurring mainly in the Bell Canyon Formation in the Delaware Basin, many species of well preserved radiolarians have been described and their assemblages have been documented (e.g. Nazarov and Ormiston, 1985, 1986a, b; Maldonado and Noble, 2010; Nestell and Nestell, 2010; Noble and Jin, 2010). Nestell and Nestell (2010) recognized the three late Capitanian radiolarian assemblages (indices) in the Bell Canyon Formation. They are the assemblages characterized by (1) *Follicucullus scholasticus* and *Tormentum sertulum*, (2) *F. orthogonus* and *Albaillella yamakitai* plus *F. sphaericus*, *F. scholasticus*, and *Ishigaum trifustis*, and (3) *Cauletella manica* and *Nazarovispongus globosum*, in ascending order. On the basis of the faunal association, we consider that the radiolarian assemblages (2) and (3) of Nestell and Nestell (2010) correspond with the *Foremanhelena triangula*, *Ruzhencevispongus* sp. B, *Ruzhencevispongus*. sp. C, and *Triplanospongos angustus* interval zones of the present study (Figure 13).

Nestell and Nestell (2010) correlated their radiolarian assemblage (2) and (3) with the *Jinogondolella altudaensis* Zone and the *Clarkina hongshuiensis* Zone, respectively. According to Zhang *et al*. (2007), who recognized the faunal transition from the *Jinogondolella*-dominated faunas in the Capitanian into the *Clarkina*-dominated faunas in the Wuchiapingian, the *Jinogondolella altudaensis* and *Clarkina hongshuiensis* zones are correlated approximately with the Guadalupian-Lopingian boundary interval, comprising the uppermost Capitanian to the lowermost Wuchiapingian. On the basis of the comparison, the age of the *Foremanhelena triangula*, *Ruzhencevispongus* sp. B, *Ruzhencevispongus*. sp. C, and *Triplanospongos angustus* interval zones is best approximated as the latest Capitanian to the earliest Wuchiapingian (Figure 13). The *Triplanospongos angustus* Interval Zone possibly includes the Guadalupian-Lopingian boundary.

Comparison with radiolarian species in GSSP section

Kuwahara *et al*. (2005) examined the radiolarians of the lowermost Heshan Formation along the Penglaitan section of Guangxi, south China, designated as Global Boundary Stratotype Section and Point for the Guadalupian-Lopingian boundary. These authors have shown that *Foremanhelena triangula* and *Triplanospongos* cf. *angustus*, nominal species for our interval zones, occur 2 m (sample R3221) and 12.4 m (sample R2214) above the base of the Heshan Formation underlain by the Capitanian Maokou Formation. The two nominal species occur in the same stratigraphic order in the Penglaitan section and our study section (Figure 12).

The Heshan Formation along the Penlaitang section is examined also in terms of the conodont biostratigraphy by several workers (e.g. Jin *et al*., 1998; Mei *et al*., 1998). These authors revealed that the 1-m-thick stratigraphic interval at the base of the Wuchiapingian is correlated with the *Clarkina postbitteri postbitteri* Zone, which is, in turn, followed by the *C. dukouensis* Zone and then the *C. asymmetrica* Zone. These zones are correlated with the lower Wuchiapingian (Jin *et al*., 1998).

On the basis of the thickness of the conodont zones in the Penglaitan section by Jin *et al*. (1998), *Foremanhelena triangula*-bearing sample R2231 is thought to be in the basal part of the *C. dukouensis* Zone, the second conodont zone from the bottom of the Wuchiapingian. As well the *Triplanospongos* cf. *angustus*-bearing sample R2214 is thought to be positioned near the boundary between the *C. dukouensis* and *C. asymmetrica* zones. The stratigraphic positions of these two samples lead to an age assignment of both samples R2231 and 2214 to the Wuchiapingian.

Our examination revealed that the continuous and abundant occurrence of *Foremanhelena triangula* is recorded from the *Foremanhelena triangula* Interval Zone up to the lower part of the *Ruzhencevispongus* sp. C Interval Zone (Figure 5), although it occurs sparsely up into the *Triplanospongos angustus* Interval Zone (Figure

12). Thus, following Nishikane *et al*. (2011) and with an emphasis on the stratigraphic intervals of the dominant occurrence, we infer that the *Foremanhelena triangula* Interval Zone and the following *Triplanospongos angustus* Interval Zone are largely correlated with the upper Capitanian (Figure 12).

The above comparison revealed a discrepancy between ages of the *Foremanhelena triangula* and *Triplanospongos angustus* interval zones inferred in our study section (late Capitanian) and their nominal species based on the conodont biostratigraphy in the Penglaitan section (early Wuchiapingian). We consider that the scattered occurrence of the two nominal species in the Penglaitan section most possibly accounts for this discrepancy. Although radiolarians are moderately preserved in the Penglaitan section, identifiable species occur sporadically, extracted from merely 6 samples out of 48 collected from the 24-m-thick section of the lowest Heshan Formation (Kuwahara *et al*., 2005). Combined with the conodont biostratigraphy, further careful examination of radiolarians in the Penglaitan section allows us more precisely to draw the correlation between the interval zones of the present study and the stratigraphic distribution of radiolarians in the GSGP section.

Conclusions

The Latentifistularia, another major group of the late Capitanian to early Wuchiapingian radiolarians, has attracted little attention as a biostratigraphic tool. Our thorough biostratigraphic examination of the Latentifistularia demonstrates their suitability for constructing an upper Capitanian to lower Wuchiapingian biostratigraphic zonation. Some species exhibit distinct stratigraphic ranges, by which we established Latentifistularia-based interval zones. Careful examination permits us to establish six latentifistularian-based interval zones. They are the *Foremanhelena triangula*, *Ruzhencevispongus* sp. B, *Ruzhencevispongus* sp. C, *Triplanospongos angustus*, *Cauletella paradoxa*, and *Triplanospongos musashiensis* interval zones, in ascending order. An unnamed zone yielding *Follicucullus charveti* and *F. bipartitus* underlies the lowest interval zone. The *Foremanhelena triangula*, *Ruzhencevispongus* sp. B, *Ruzhencevispongus* sp. C, *Triplanospongos angustus* interval zones are correlated with the *Follicucullus charveti-Albaillella yamakitai* and the *Cauletella paradoxa* and *Triplanospongos musashiensis* interval zones are correlated with the *Neoalbaillella ornithoformis* Assemblage Zone in Japan. The *Foremanhelena triangula*, *Ruzhencevispongus* sp. B, *Ruzhencevispongus* sp. C interval zones and the lower part of the *Triplanospongos angustus* Interval Zone are compared with the *Follicucullus orthogonus-Albaillella yamakitai* and *Cauletella manica-Nazarovispongus globosum* radiolarian indices in North America, and also with the *Follicucullus charveti and Albaillella levis* assemblage in South China. We infer that the *Foremanhelena triangula*, *Ruzhencevispongus* sp. B, and *Ruzhencevispongus* sp. C interval zones and the *Cauletella paradoxa* and *Triplanospongos musashiensis* interval zones are compared with the upper Capitanian and lower Wuchiapingian, respectively. The *Triplanospongos angustus* Interval Zone presumably includes the Guadalupian-Lopingian boundary. We emphasize the significant availability of the Latentifistularia for the upper Capitanian to lower Wuchiapingian biostratigraphic zonation, even if the Albaillellaria are poor.

Acknowledgements

We express our special thanks to the late T. Kunishima (Gifu City), the landowner of the Iwaidani gully, for granting his special permission for our fieldwork, and M. Murai (Motosu City), the manager of the Iwaidani gully logging road, who offered us facilities for fieldwork. Our sincere thanks go to Paula Noble (University of Nevada, Reno) for her linguistic and scientific reviews on the early version of the manuscript. A suggestion by A. Takemura (Hyogo University of Teacher Education) and an anonymous reviewer of the journal much improved the manuscript. Part of our research was financially supported by Grants-in-Aid for Scientific Research of the Japan Society for the Promotion of Science (Project/Area Numbers JP23540552 and JP16K13899 to the first author and JP24540499 to the second author).

References

Caridroit, M. and De Wever, P., 1986: Some Late Permian radiolarians from pelitic rocks of the Tatsuno Formation (Hyogo Prefecture), southwest Japan. *Marine Micropaleontology*, vol. 11, p. 55–90.

Feng, Q., He, W., Gu, S., Jin, Y. and Meng, Y., 2006a: Latest Permian Spumellaria and Entactinaria (Radiolaria) from south China. *Revue de Micropaléontologie*, vol. 49, p. 21–43.

Feng, Q., He, W., Zhang, S. and Gu, S., 2006b: Taxonomy of order Latentifistularia (Radiolaria) from the latest Permian in Southern Guangxi, China. *Journal of Paleontology*, vol. 80, p. 826–848.

Holdsworth, B. K. and Jones, D. L., 1980: Preliminary radiolarian zonation for Late Devonian through Permian time. *Geology*, vol. 8, p. 281–285.

Ishiga, H., 1986: Late Carboniferous and Permian radiolarian biostratigraphy of Southwest Japan. *Journal of Geoscience*, *Osaka City University*, vol. 29, p. 89–100.

Ishiga, H. and Imoto, N., 1980: Some Permian radiolarians in the Tamba district, Southwest Japan. *Earth Science (Chikyu Kagaku)*, vol. 34, p. 333–345.

Ishiga, H., Kito, T. and Imoto, N., 1982: Permian radiolarian biostratigraphy. *News of Osaka Micropaleontologists*, *Special Volume*, no. 5, p. 17–26.

Jin, Y., Mei, S., Wang, W., Wang, X., Shen, S., Shang, Q. and Chen, Z., 1998: On the Lopingian Series of the Permian System. *Palaeoworld*, no. 9, p. 1–18.

Jones, G., Valsami-Jones, E. and Sano, H., 1993: Nature and tectonic setting of accreted basalts from the Mino terrane, central Japan. *Journal of Geological Society of London*, vol. 150, p. 1167–1181.

Kitao, K., 1996: Middle and Upper Permian conodont biostratigraphy in bedded cherts of the Mino terrane, central Japan. *Journal of Geosciences*, *Osaka City University*, vol. 39, p. 61–81.

Kozur, H., 1980: Ruzhencevispongidae, eine neue Spumellaria-Familie aus dem oberen Kungurian (Leonardian) und Sakmarian des Vorurals. *Geologische-Paläontologische Mitteilungen Innsbruck*, Band 10, S. 235–242.

Kuwahara, K., 1997: Upper Permian radiolarian biostratigraphy: Abundance zones of *Albaillella. News of Osaka Micropaleontologists*, *Special Volume*, no. 10, p. 55–75. (*in Japanese with English abstract*)

Kuwahara, K., 1999: Phylogenetic lineage of Late Permian *Albaillella* (Albaillellaria, Radiolaria). *Journal of Geosciences*, *Osaka City University*, vol. 42, p. 85–101.

Kuwahara, K., Sano, H., Yao, A. and Ezaki, Y., 2010: Discovery of Triassic siliceous rocks from within large Permian oceanic-rock mass in the Mt. Funabuseyama area of the western part of Mino terrane and its geologic implication. *Journal of Geological Society of Japan*, vol. 116, p. 159–173. (*in Japanese with English abstract*)

Kuwahara, K., Yao, A. and Yamakita, S., 1998: Reexamination of Upper Permian radiolarian biostratigraphy. *Earth Science (Chikyu Kagaku)*, vol. 52, p. 391–404.

Kuwahara, K., Yao, A., Yao, J. and Li, J., 2005: Permian radiolarians from the Global Boundary Stratotype Section and Point for the Guadalupian-Lopingian boundary in the Laibin area, Guangxi, China. *Journal of Geosciences*, *Osaka City University*, vol. 48, p. 95–107.

Maldonado, A. L. and Noble, P. J., 2010: Radiolarians from the upper Guadalupian (Middle Permian) Reef Trail Member of the Bell Canyon Formation, West Texas and their biostratigraphic implications. *Micropaleontology*, vol. 56, p. 69–115.

Mei, S., Jin, Y. and Wardlaw, B. R., 1998: Conodont succession of the Guadalupian-Lopingian boundary strata in Laibin of Guangxi, China and West Texas, USA. *Palaeoworld*, no. 9, p. 53–76.

Mizutani, S., 1990: Mino Terrane. *In*, Ichikawa, K., Mizutani, S., Hada, S. and Yao, A. *eds*., *Pre-Cretaceous Terranes of Japan*, p. 121–135. Publication of International Geological Correlation Project No. 224, Osaka.

Nazarov, B. B. and Ormiston, A. R., 1985: Radiolaria from the Late Paleozoic of Southern Urals, USSR and West Texas, USA. *Micropaleontology*, vol. 31, p. 1–54.

Nazarov, B. B. and Ormiston, A. R., 1986a: Trends in the development of Paleozoic Radiolaria. *Marine Micropaleontology*, vol. 11, p. 3–32.

Nazarov, B. B. and Ormiston, A. R., 1986b: Origin and biostratigraphic potential of the stauraxon polycystine Radiolaria. *Marine Micropaleontology*, vol. 11, p. 33–54.

Nestell, G. P. and Nestell, M. K., 2010: Late Capitanian (latest Guadalupian, Middle Permian) radiolarians from the Apache Mountains, West Texas. *Micropaleontology*, vol. 56, p. 7–68.

Nishikane, Y., Kaiho, K., Takahashi, S., Henderson. C. M., Suzuki, N. and Kanno, M., 2011: The Guadalupian-Lopingian boundary (Permian) in a pelagic sequence from Panthalassa recognized by integrated conodont and radiolarian biostratigraphy. *Marine Micropaleontology*, vol. 78, p. 84–95.

Noble, J. P. and Jin, Y., 2010: Radiolarians from the Lamar Limestone, Guadalupe Mountains, West Texas. *Micropaleontology*, vol. 56, p. 117–147.

Noble, P. and Renne, P., 1990: Paleoenvironmental and biostratigraphic significance of siliceous microfossils of the Permo-Triassic Redding section, eastern Klamath Mountains, California. *Marine Micropaleontology*, vol. 15, p. 379–391.

Ormiston, A. and Babcock, L., 1979: *Follicucullus*, new radiolarian genus from the Guadalupian (Permian) Lamar Limestone of the Delaware Basin. *Journal of Paleontology*, vol. 53, p. 328–334.

Saesaengseerung, D., Agematsu, S., Sashida, K. and Sardsud, A., 2009: Discovery of Lower Permian radiolarian and conodont faunas from the bedded chert of the Chanthaburi area along the Sra Kaeo suture zone, eastern Thailand. *Paleontological Research*, vol. 13, p. 119–138.

Safonova, I., Maruyama, S., Kojima, S., Komiya, T., Krivonogov, S. and Koshida, K., 2016: Recognizing OIB and MORB in accretionary complexes; A new approach based on oceanic plate stratigraphy, petrology and geochemistry. *Gondwana Research*, vol. 33, p. 92–114.

Sano, H., 1988a: Permian oceanic-rocks of Mino terrane, central Japan. Part I. chert facies. *Journal of the Geological Society of Japan*, vol. 94, p. 697–709.

Sano, H., 1988b: Permian oceanic-rocks of Mino terrane, central Japan. Part II. limestone facies. *Journal of the Geological Society of Japan*, vol. 94, p. 963–976.

Sano, H., 1989a: Permian oceanic-rocks of Mino terrane, central Japan. Part III. limestone-breccia facies. *Journal of the Geological Society of Japan*, vol. 95, p. 527–540.

Sano, H., 1989b: Permian oceanic-rocks of Mino terrane, central Japan. Part IV. Supplements and concluding remarks. *Journal of the Geological Society of Japan*, vol. 95, p. 595–602.

Sano, H., Kuwahara, K., Yao, A. and Agematsu, S., 2010: Panthalassan seamount-associated Permian-Triassic boundary siliceous rocks, Mino terrane, central Japan. *Paleontological Research*, vol. 14, p. 295–316.

Sano, H., Kuwahara, K., Yao, A. and Agematsu, S., 2012: Stratigraphy and age of the Permian-Triassic boundary siliceous rocks of the Mino terrane in the Mt. Funabuseyama area, central Japan. *Paleontological Research*, vol. 16, p. 124–145.

Sano, H., Yamagata, T. and Horibo, K., 1992: Tectonostratigraphy of Mino terrane: Jurassic accretionary complex of southwest Japan. *Palaeogeography*, *Palaeoclimatology*, *Palaeoecology*, vol. 96, p. 41–57.

Sashida, K. and Tonishi, K., 1985: Permian radiolarians from the Kanto Mountains, Central Japan—some Upper Permian Spumellaria from Itsukaichi, western part of Tokyo Prefecture—. *Science Reports of the Institute of Geoscience*, *University of Tsukuba*, *Section B*, *Geological Sciences*, vol. 6, p. 1–19.

Sashida, K. and Tonishi, K., 1986: Upper Permian stauraxon polycystine radiolaria from Itsukaichi, western part of Tokyo Prefecture. *Science Reports of the Institute of Geoscience*, *University of Tsukuba*, *Section B*, *Geological Sciences*, vol. 7, p. 1–13.

Sashida, K. and Tonishi, K., 1988: Additional note on Upper Permian radiolarian fauna from Itsukaichi, western part of Tokyo Prefecture, central Japan. *Transactions and Proceedings of the Palaeontological Society of Japan*, *New Series*, no. 151, p. 523–542.

Shang, Q., Caridroit, M. and Wang, Y., 2001: Radiolarians from the uppermost Permian Changhsingian of southern Guangxi. *Acta Micropalaeontologica Sinica*, vol. 18, p. 229–240.

Sun, D. and Xia, W., 2006: Identification of the Guadalupian–Lopingian boundary in the Permian in a bedded chert sequence, South China. *Palaeogeography*, *Palaeoclimatology*, *Palaeoecology*, vol. 236, p. 272–289.

Wakita, K., 1988: Origin of chaotically mixed rock bodies in the Early Jurassic to Early Cretaceous sedimentary complex of the Mino terrane, central Japan. *Bulletin of the Geological Survey of Japan*, vol. 39, p. 675–757.

Wakita, K., 2012: Mappable features of mélanges derived from Ocean Plate Stratigraphy in the Jurassic accretionary complexes of Mino and Chichibu terranes in Southwest Japan. *Tectonophysics*, vols. 568 and 569, p. 74–85.

Wang, Y., Luo, H. and Yang, Q., 2012: Late Paleozoic radiolarians in the Qingfang area, southwest Guangxi. *University of Science and Technology of China Press*, 127 p. (*in Chinese with English abstract*)

Wang, Y. and Yang, Q., 2011: Biostratigraphy, phylogeny and paleobiogeography of Carboniferous–Permian radiolarians in South China. *Palaeoworld*, vol. 20, p. 134–145.

Wang, Y., Yang, Q., Cheng, Y. and Li, J., 2006: Lopingian (Upper Permian) radiolarian biostratigraphy of South China. *Palaeoworld*, vol. 15, p. 31–53.

Xia, W., Zhang, N., Kakuwa, Y. and Zhang, L., 2005: Radiolarian and conodont biozonation in the pelagic Guadalupian-Lopingian boundary interval at Dachongling, Guangxi, South China, and mid-upper Permian global correlation. *Stratigraphy*, vol. 2, p. 217–238.

Xia, W., Zhang, N., Wang, G. and Kakuwa, Y., 2004: Pelagic radiolarian and conodont biozonation in the Permo-Triassic boundary interval and correlation to the Meishan GSSP. *Micropaleontology*, vol. 50, p. 27–44.

Zhang, L., Zhang, N. and Xia, W., 2007: Conodont succession in the Guadalupian-Lopingian boundary interval (upper Permian) of the Maoershan section, Hubei Province, China. *Micropaleontology*, vol. 53, p. 433–446.